doi: 10.1038/nature07473

Deconstructing voltage sensor function and pharmacology in sodium channels

Frank Bosmans, Marie-France Martin-Eauclaire and Kenton J. Swartz

a

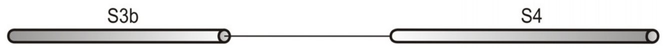


```
Kv2.1           FFKGPLNAIDLLAILPY-YVTIFLTESNKSVLQFQNVRRVVQIFRIMRILRILKLARHSTGLQS
rNav1.2a DI     FLRNPWNWLDFTVITFA-YVTEFVNLGN------------VSALRTFRVLRALKTISVIPGLKT
rNav1.4 DI      FLRNPWNWLDFSVITMA-YVTEFVDLGN------------ISALRTFRVLRALKTITVIPGLKT
                FFKGPLNAIDLLAILTFAYVTEFVNLGN------------VSALRTFRVLRILKLARHSTGLQS*
                FFKGPLNAIDLLAITFA-YVTEFVNLGN------------VSALRTFRVLRILKLARHSTGLQS   DI
                FFKGPLNAIDLLAITMA-YVTEFVDLGN------------ISALRTFRVLRILKLARHSTGLQS

Kv2.1           FFKGPLNAIDLLAI-LPYYVTIFLTESNKSVLQFQNVRRVVQIFRIMRILRILKLARHSTGLQS
rNav1.2a DII    YFQEGWNIFDGFIV-SLSLMELGLANVE-----------GLSVLRSFRLLRVFKLAKSWPTLNM
rNav1.4 DII     YFQEGWNIFDSIIV-TLSLVELGLANVQ-----------GLSVLRSFRLLRVFKLAKSWPTLNM
                FFKGPLNAIDLLAILSLSLMELGLANVE-----------GLSVLRSFRLLRILKLARHSTGLQS*
                FFKGPLNAIDLLAI-SLSLMELGLANVE-----------GLSVLRSFRLLRILKLARHSTGLQS   DII
                FFKGPLNAIDLLAI-TLSLVELGLANVQ-----------GLSVLRSFRLLRILKLARHSTGLQS

Kv2.1           FFKGPLNAIDLLAILPYYVTIFLTESNKSVLQFQNVRRVVQIFRIMRILRILKLARHSTGLQS
rNav1.2a DIII   YFTNAWCWLDFLIVDVSLVSLTANALGYSEL------GAIKSLRTLRALRPLRALSRFEGMRV
rNav1.4 DIII    YFTNAWCWLDFLIVDVSIISLVANWLGYSEL---------GPIKSLRTLRALRPLRALSRFEG
                FFKGPLNAIDLLAIL-SLVSLTANALGYSEL------GAIKSLRTLRALRILKLARHSTGLQS*
                FFKGPLNAIDLLAILPSLVSLTANALGYSEL---------GAIKSLRTLRALRLARHSTGLQS   DIII
                FFKGPLNAIDLLAILPSIISLVANWLGYSEL---------GPIKSLRTLRALRLARHSTGLQS

Kv2.1           FFKGPLNAIDLLAILPYYVTIFLTESNKSVLQFQNVRRVVQIFRIMRILRILKLARHSTGLQS
rNav1.2a DIV    YFTIGWNIFDFVVVILSIVGMFLAELIEKYFVSPTLFRVIRLARIGRILRLIKGAKGIRTLLF
rNav1.4 DIV     YFTIGWNIFDFVVVILSIVGLALSDLIQKYFVSP---TLFRVIRLARIGRVLRLIRGAKGIRT
                FFKGPLNAIDLLAIL-SIVGMFLAELIEKYFVSPTLFRVIRLARIGRILRILKLARHSTGLQS
                FFKGPLNAIDLLAILLSIVGMFLAELIEKYFVSPTLFRVIRLARIGRILRILKLARHSTGLQS
                FFKGPLNAIDFVVVILSIVGMFLAELIEKYFVSPTLFRVIRLARIGRILRILKLARHSTGLQS
                FFKGPLNAIDLLAILLSIVGMFLAELIEKYFVSP---TLFRVIRLARIGRILRLARHSTGLQS*
                FFKGPLNAIDLLAILPSIVGMFLAELIEKYFVSP---TLFRVIRLARIGRILRLARHSTGLQS   DIV
                FFKGPLNAIDLLAILPSIVGLALSDLIQKYFVSP---TLFRVIRLARIGRVLRLARHSTGLQS
```

b

```
Kv1.3           FSRNIMNLIDIVAIIPYFITLGTELAERQGNGQQAMSLAILRVIRLVRVFRIFKLSRHSKGLQI
rNav1.4a DI     FLRNPWNWLDFTVITMAYVTEFVDLGN-------------ISALRTFRVLRALKTISVIPGLKT
rNav1.4a DII    YFQEGWNIFDGFIVTLSLVELGLANVQ------------GLSVLRSFRLLRVFKLAKSWPTLNM
rNav1.4a DIII   YFTNAWCWLDFLIVDVSIISLVANWLGYSEL----------GPIKSLRTLRALRPLRALSRFEV
rNav1.4a DIV    YFTIGWNIFDFVVVILSIVGLALSDLIQKYFVSP----TLFRVIRLARIGRVLRLIKGAKGIRL
```

c

```
Shaker          MNVIDIIAIIPYFITLATVVAEEEDTLNLPKAPVSPQDKSSNQAMSLAILRVIRLVRVFRIFKLSRHSK
rNav1.4a DI     WNWLDFTVITMAYVTEFVDLGN---------------------------ISALRTFRVLRALKTISVIP
rNav1.4a DII    WNIFDGFIVTLSLVELGLANVQ--------------------------GLSVLRSFRLLRVFKLAKSWP
rNav1.4a DIII   WCWLDFLIVDVSIISLVANWLGYSEL------------------------GPIKSLRTLRALRPLRALS
rNav1.4a DIV    WNIFDFVVVILSIVGLALSDLIQKYFVSP------------------TLFRVIRLARIGRVLRLIKGAK
```

d

		%Id	%Co
HaTx	--E**C**RYLFGG**C**K--TTSD**CC**KHLG-**C**KFRDKY**C**AWDFTFS		
SGTx1	--T**C**RYLFGG**C**K--TTAD**CC**KHLA-**C**RSDGKY**C**AWDGTF-	76	82
ProTx-I	--E**C**RYWLGG**C**S--AGQT**CC**KHLV-**C**SRRHGW**C**VWDGTFS	57	60
VSTX1	--E**C**GKFMWK**C**K--NSND**CC**KDLV-**C**SSRWKW**C**VLASPF-	41	50
PaurTx3	--D**C**LGFLWK**C**NPSND-K**CC**RPNLV**C**SRKDKW**C**KYQI---	26	42
ProTx-II	--Y**C**QKWMWT**C**DS--ERK**CC**EGMV-**C**R---LW**C**KKKLW--	21	38
GxTx-1E	EGE**C**GGFWWK**C**G-SGKPA**CC**PKYV-**C**SPKWGL**C**NFPMP--	21	30

Supplementary Figure 1: Defining the paddle chimaeras. a, Sequence alignment of the paddle region of Kv2.1 with the separate S3b-S4 regions of rNav1.2a and rNav1.4 arranged per domain. Only chimaeras that produce functional channels are shown. Arrows indicate chimaeras that were used for experiments described in the main text. Asterisks demarcate additional chimaeras for which data are reported in Supplementary Table 1. **b,c,** Sequence alignment of the paddle region of Kv1.3 and Shaker with the separate S3b-S4 regions of rNav1.2a. Colored regions were transferred into the Kv channel and are purple for DI, red for DII, blue for DIII and green for DIV. **d,** Sequence alignment of spider toxins used in this work. Id = Identity, Co = Conserved, relative to HaTx.

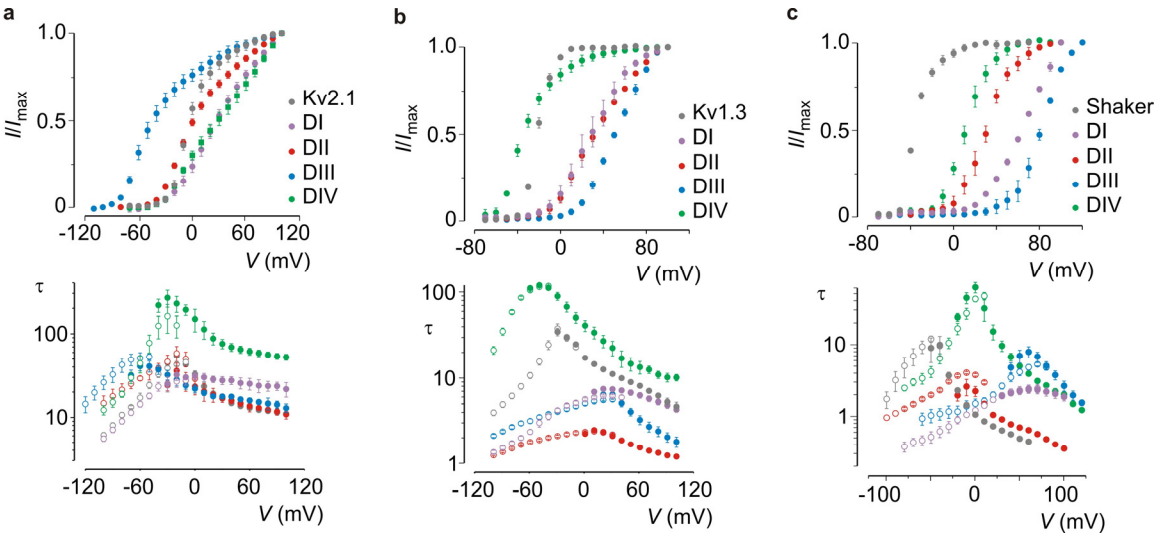

Supplementary Figure 2: Gating properties for rNav1.4/Kv2.1, rNav1.4/Kv1.3 and rNav1.4/Shaker chimaeras. Voltage-activation relationships (top) and kinetics of opening and closing (bottom) for chimaeras containing paddle motifs from the four domains of rNav1.4 in Kv2.1 **(a)**, Kv1.3 **(b)** and Shaker **(c)** Kv channels. I/I_{max} is normalized tail current amplitude, plotted as a function of voltage (V). Mean time constants (τ) from single exponential fits to channel activation (filled circles) and deactivation (open circles) plotted as a function of the voltage at which the current was recorded. n = 4-8 and error bars represent s.e.m.

Construct	$V_{1/2}$ (mV)	z
Kv2.1	0 ± 1	2.7 ± 0.2
DI (rNav1.2a)	48 ± 1	1.8 ± 0.1
DII (rNav1.2a)	29 ± 1	1.6 ± 0.1
DIII (rNav1.2a)	5 ± 1	1.2 ± 0.1
DIV (rNav1.2a)	23 ± 1	1.7 ± 0.1
DI (rNav1.2a) *	11 ± 1	2.4 ± 0.1
DII (rNav1.2a) *	47 ± 1	2.7 ± 0.1
DIII (rNav1.2a) *	10 ± 1	1.5 ± 0.1
DIV (rNav1.2a)*	42 ± 1	2.6 ± 0.1
DI (rNav1.4)	29 ± 1	1.7 ± 0.1
DII (rNav1.4)	7 ± 2	1.7 ± 0.1
DIII (rNav1.4)	-36 ± 3	1.5 ± 0.1
DIV (rNav1.4)	30 ± 2	1.5 ± 0.1

Supplementary Table 1: Gating properties of rNav1.2a/rNav1.4 and Kv2.1 chimaeras. Midpoint (mV) and slope (z) values obtained by fitting voltage-activation relations with single Boltzmann functions. n=5-18 and errors are s.e.m. Asterisks identify chimaeras indicated by asterisks in Supplementary Fig. 1.

Construct	$V_{1/2}$ (mV)	z
Shaker	-34 ± 1	5.0 ± 0.5
DI (rNav1.4)	> +50[a]	-
DII (rNav1.4)	30 ± 1	3.0 ± 0.1
DIII (rNav1.4)	> +50[a]	-
DIV (rNav1.4)	11 ± 1	3.4 ± 0.1
Kv1.3	-21 ± 1	6.0 ± 0.2
DI (rNav1.4)	29 ± 1	2.2 ± 0.1
DII (rNav1.4)	33 ± 1	2.0 ± 0.1
DIII (rNav1.4)	51 ± 1	2.6 ± 0.1
DIV (rNav1.4)	-31 ± 1	2.7 ± 0.2

Supplementary Table 2: Gating properties of the chimaeras between rNav1.4 and Shaker and Kv1.3. Values are as in Supplementary Table 1. n=3-5 and errors are s.e.m. [a]These channels have G-V relationships that do not saturate at voltages up to +100 mV.

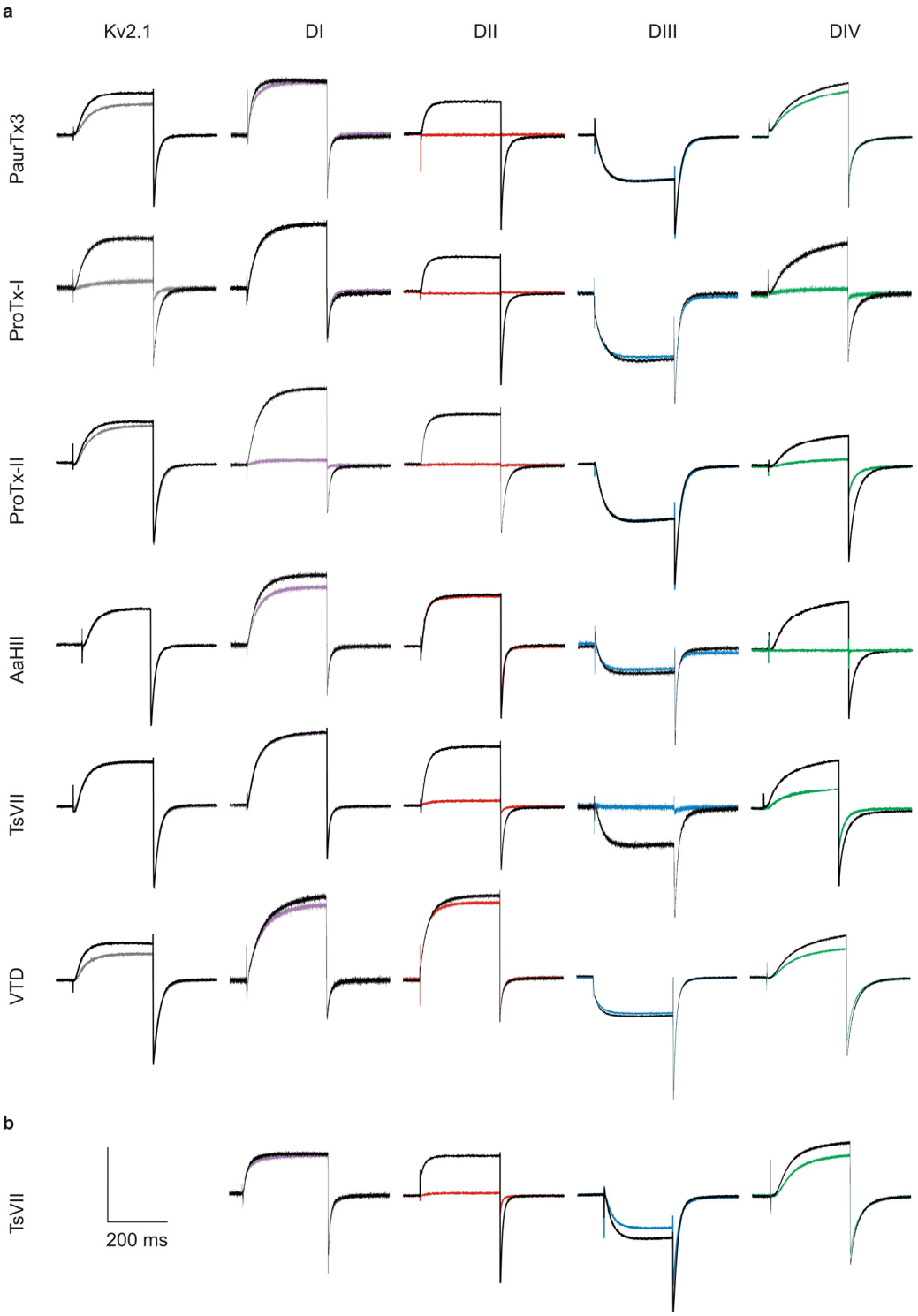

Supplementary Figure 3: Chimaera currents in the absence and presence of toxins. a, Potassium currents elicited by depolarizations near the foot of the voltage-activation curve (see Fig. 2) for Kv2.1 and rNav1.2a/Kv2.1 chimaeras. Currents are shown before (black) and in the presence of toxin. Data are grouped per toxin (horizontally) and per chimaera (vertically). Concentrations used are 100nM PaurTx3, ProTx-I and ProTx-II; 1μM AaHII; 500nM TsVII and 100μM VTD (=veratridine). **b,** Data represent 50nM TsVII on rNav1.4/Kv2.1 chimaeras.

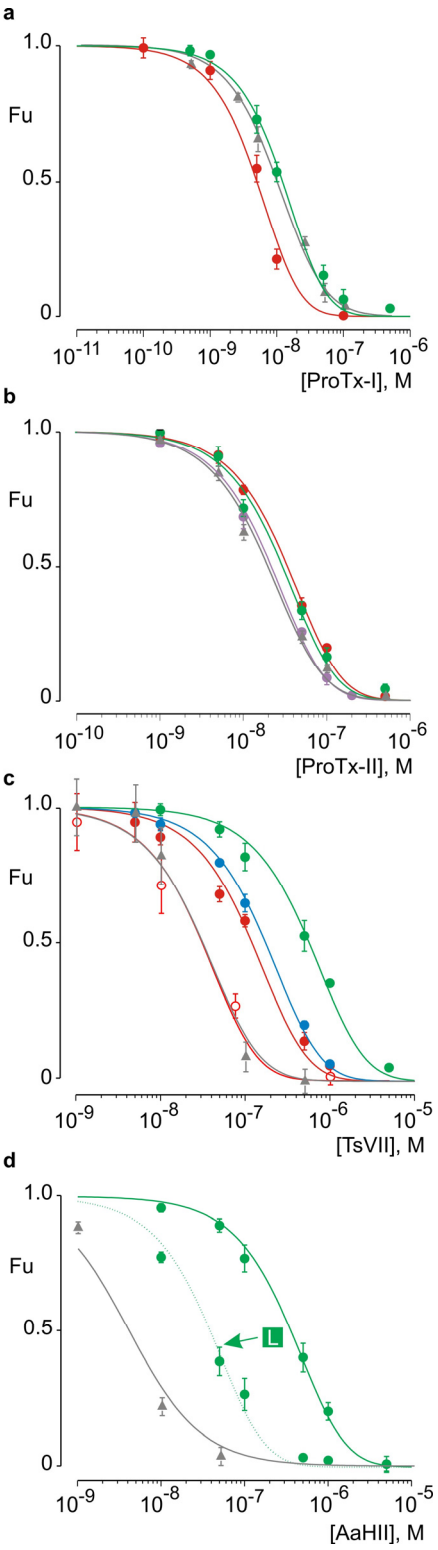

a Paddle chimaeras - four site model Kd, nM

Toxin	DI	DII	DIII	DIV
PaurTx3	nd	8 ± 1	nd	nd
ProTx-I	nd	27 ± 3	nd	66 ± 5
ProTx-II	114 ± 6	118 ± 8	nd	155 ± 14
AaHII	nd	nd	nd	1902 ± 102
TsVII	nd	643 ± 70	929 ± 40	3038 ± 236
TsVII[a]	nd	163 ± 28	nd	nd

b Paddle chimaeras - Hill equation Kd, nM

Toxin	DI	DII	DIII	DIV
PaurTx3	nd	2 ± 1 (*1.3*)	nd	nd
ProTx-I	nd	5 ± 1 (*1.2*)	nd	12 ± 1 (*1.2*)
ProTx-II	19 ± 2 (*1.2*)	30 ± 1 (*1.2*)	nd	26 ± 2 (*1.2*)
AaHII	nd	nd	nd	319 ± 21 (*1.1*)
TsVII	nd	112 ± 12 (*1.1*)	157 ± 9 (*1.2*)	527 ± 37 (*1.0*)
TsVII[a]	nd	26 ± 1 (*1.0*)	nd	nd

c rNav1.2a - variable site models

Toxin	Kd, nM	*n*	Kd, nM	*n*
PaurTx3	30 ± 2	*1.1*	29 ± 4	*1*
ProTx-I	17 ± 2	*1.2*	46 ± 3	2
ProTx-II	17 ± 1	*1.2*	74 ± 7	3
AaHII	5 ± 1	*1.5*	6 ± 2	1
TsVII	25 ± 4	*1.8*	121 ± 25	3

Supplementary Table 3: Apparent K_d values for toxin interaction with paddle chimaeras and the rNav1.2a channel. K_d values for toxins interacting with Nav channel paddle chimaeras obtained by fitting the concentration-dependence for toxin inhibition of channel opening in response to weak depolarizations with a four site model **(a)** or the Hill equation **(b)** with Hill coefficients (*n*) given in parentheses. [a]These values were obtained with the rNav1.4 paddle chimaera. For the four site model, fraction unbound (Fu) = $(1-[Toxin]/([Toxin] + K_d))^4$, while in the Hill equation Fu = $(1-[Toxin]^n / ([Toxin]^n + K_d^n)$. **c,** K_d values for toxins interacting with rNav1.2a obtained using the Hill equation (left) or equations specifying 1 to 3 binding sites where occupancy of any one site is sufficient to inhibit opening. In these cases, Fu = $(1-[Toxin]/([Toxin] + K_d))^n$.

Supplementary Figure 4: Apparent affinities for extracellular toxins interacting with rNav1.2a paddle chimaeras. a-d, Concentration dependence for toxin inhibition plotted as fraction unbound (Fu) measured at negative voltages for ProTx-I on DII and DIV **(a)**, ProTx-II on DI, DII and DIV **(b)**, TsVII on DII, DIII and DIV **(c)** and AaHII on DIV and the L1630A mutant indicated with a green arrow and dotted line **(d)**. All rNav1.2a paddle chimaera data are shown with solid symbols, while that for the rNav1.2a channel are shown with solid gray triangles. Data for the DII rNav1.4 paddle chimaera are shown in **c** using open red circles. Lines represent a fit with Fu = $([Toxin]/([Toxin] + K_d))^4$, assuming four independent toxin binding sites per channel, while those for the rNav1.2a channel represent Hill equation fits with 1 to 3 sites per channel (see Supplementary Table 3). n = 3-5 for each toxin concentration and error bars represent s.e.m.

Mutant	$V_{1/2}$ (mV)	z
T1A	32 ± 1	1.6 ± 0.1
F2A	26 ± 1	1.6 ± 0.1
A3V	> +50[a]	-
Y4A	29 ± 2	1.5 ± 0.1
V5A	36 ± 2	1.5 ± 0.1
T6A	> +50[a]	-
E7A	> +50[a]	-
E7K	> +50[a]	-
F8A	> +50[a]	-
V9A	> +50[a]	-
D10A	> +50[a]	-
L11A	> +50[a]	-
G12A	38 ± 1	1.6 ± 0.1
N13A	38 ± 1	1.8 ± 0.1
V14A	20 ± 1	1.5 ± 0.1
S15A	35 ± 1	1.6 ± 0.1
A16V	37 ± 1	1.7 ± 0.1
L17A	45 ± 2	1.5 ± 0.1
R18A	-	-
T19A	-12 ± 2	1.2 ± 0.1
F20A	> +50[a]	-
R21A	22 ± 1	1.7 ± 0.1
V22A	> +50[a]	-
L23A	> +50[a]	-
R24A	22 ± 1	1.7 ± 0.1

Supplementary Table 4: Gating properties of the DI chimaeras between rNav1.2a/Kv2.1. Values are as in Supplementary Table 1. n=3-5 and errors are s.e.m. [a]These channels have G-V relationships that do not saturate at voltages up to +100 mV.

Mutant	$V_{1/2}$ (mV)	z
S1A	14 ± 1	1.6 ± 0.1
L2A	21 ± 2	1.4 ± 0.1
S3A	23 ± 1	1.6 ± 0.1
L4A	31 ± 1	2.0 ± 0.1
M5A	15 ± 2	1.6 ± 0.1
E6A	6 ± 1	1.9 ± 0.1
L7A	17 ± 1	1.6 ± 0.1
G8A	12 ± 1	1.6 ± 0.1
L9A	40 ± 1	1.9 ± 0.1
A10V	35 ± 1	2.0 ± 0.1
N11A	35 ± 1	1.8 ± 0.1
N11D	12 ± 2	1.6 ± 0.1
V12A	16 ± 1	1.6 ± 0.1
E13A	30 ± 1	1.6 ± 0.1
E13K	42 ± 2	1.6 ± 0.1
G14A	28 ± 1	1.6 ± 0.1
L15A	-2 ± 2	1.6 ± 0.1
S16A	24 ± 1	1.7 ± 0.1
V17A	29 ± 1	1.5 ± 0.1
L18A	> +50[a]	-
R19A	27 ± 1	1.5 ± 0.1
S20A	24 ± 1	1.4 ± 0.1
F21A	8 ± 2	1.0 ± 0.1
R22A	16 ± 2	1.4 ± 0.1
L23A	-8 ± 2	0.9 ± 0.1
L24A	18 ± 1	1.7 ± 0.1
R25A	15 ± 2	1.1 ± 0.1

Supplementary Table 5: Gating properties of the DII chimaeras between rNav1.2a/Kv2.1. Values are as in Supplementary Table 1. n=3-5 and errors are s.e.m. [a]These channels have G-V relationships that do not saturate at voltages up to +100 mV.

Mutant	$V_{1/2}$ (mV)	z
S1A	17 ± 2	0.9 ± 0.1
L2A	-20 ± 4	0.9 ± 0.1
V3A	-8 ± 1	1.3 ± 0.1
S4A	10 ± 2	1.4 ± 0.1
L5A	2 ± 2	1.3 ± 0.1
T6A	-12 ± 3	1.2 ± 0.1
A7V	-26 ± 2	1.5 ± 0.1
N8A	-26 ± 2	1.2 ± 0.1
A9V	-28 ± 1	1.6 ± 0.1
L10A	-7 ± 2	1.3 ± 0.1
G11A	28 ± 1	1.6 ± 0.1
Y12A	-4 ± 2	1.3 ± 0.1
S13A	-10 ± 2	1.3 ± 0.1
E14A	15 ± 1	1.7 ± 0.1
L15A	-30 ± 2	1.3 ± 0.1
G16A	-22 ± 2	1.4 ± 0.1
A17V	-16 ± 1	1.2 ± 0.1
I18A	15 ± 1	1.6 ± 0.1
K19A	-52 ± 3	1.2 ± 0.1
S20A	-15 ± 2	1.2 ± 0.1
L21A	-18 ± 2	1.4 ± 0.1
R22A	-10 ± 1	1.1 ± 0.1
T23A	13 ± 3	0.9 ± 0.1
L24A	-68 ± 1	2.7 ± 0.1
R25A	7 ± 2	0.9 ± 0.1
A26V	-14 ± 2	0.8 ± 0.1
L27A	> +50[a]	-
R28A	18 ± 2	1.0 ± 0.1

Supplementary Table 6: Gating properties of the DIII chimaeras between rNav1.2a/Kv2.1. Values are as in Supplementary Table 1. n=3-5 and errors are s.e.m. [a]These channels have G-V relationships that do not saturate at voltages up to +100 mV.

Mutant	$V_{1/2}$ (mV)	z
S1A	-1 ± 2	1.6 ± 0.1
I2A	-3 ± 2	1.9 ± 0.2
V3A	8 ± 2	2.0 ± 0.2
G4A	-6 ± 2	1.9 ± 0.2
M5A	24 ± 2	1.6 ± 0.1
F6A	18 ± 1	1.6 ± 0.1
L7A	24 ± 1	2.3 ± 0.1
A8V	16 ± 2	1.7 ± 0.1
E9A	7 ± 2	1.4 ± 0.1
L10A	34 ± 1	2.2 ± 0.1
I11A	17 ± 2	1.4 ± 0.1
E12A	24 ± 1	1.8 ± 0.1
K13A	23 ± 1	2.0 ± 0.1
Y14A	19 ± 1	1.4 ± 0.1
F15A	30 ± 1	1.6 ± 0.1
V16A	24 ± 2	1.5 ± 0.1
S17A	15 ± 1	1.9 ± 0.1
P18A	32 ± 1	2.4 ± 0.1
T19A	28 ± 2	1.9 ± 0.1
L20A	22 ± 2	1.8 ± 0.1
F21A	-	-
R22A	27 ± 1	1.5 ± 0.1
V23A	30 ± 1	2.0 ± 0.1
I24A	> +50[a]	-
R25A	10 ± 2	1.1 ± 0.1
L26A	-34 ± 3	1.3 ± 0.1
A27V	29 ± 2	1.5 ± 0.1
R28A	20 ± 1	1.2 ± 0.1
I29A	> +50[a]	-
G30A	34 ± 2	1.5 ± 0.1
R31A	32 ± 2	1.3 ± 0.1
I32A	-	-
L33A	46 ± 1	2.0 ± 0.1
R34A	> +50[a]	-

Supplementary Table 7: Gating properties of the DIV chimaeras between rNav1.2a/Kv2.1. Values are as in Supplementary Table 1. n=3-5 and errors are s.e.m. [a]These channels have G-V relationships that do not saturate at voltages up to +100 mV.

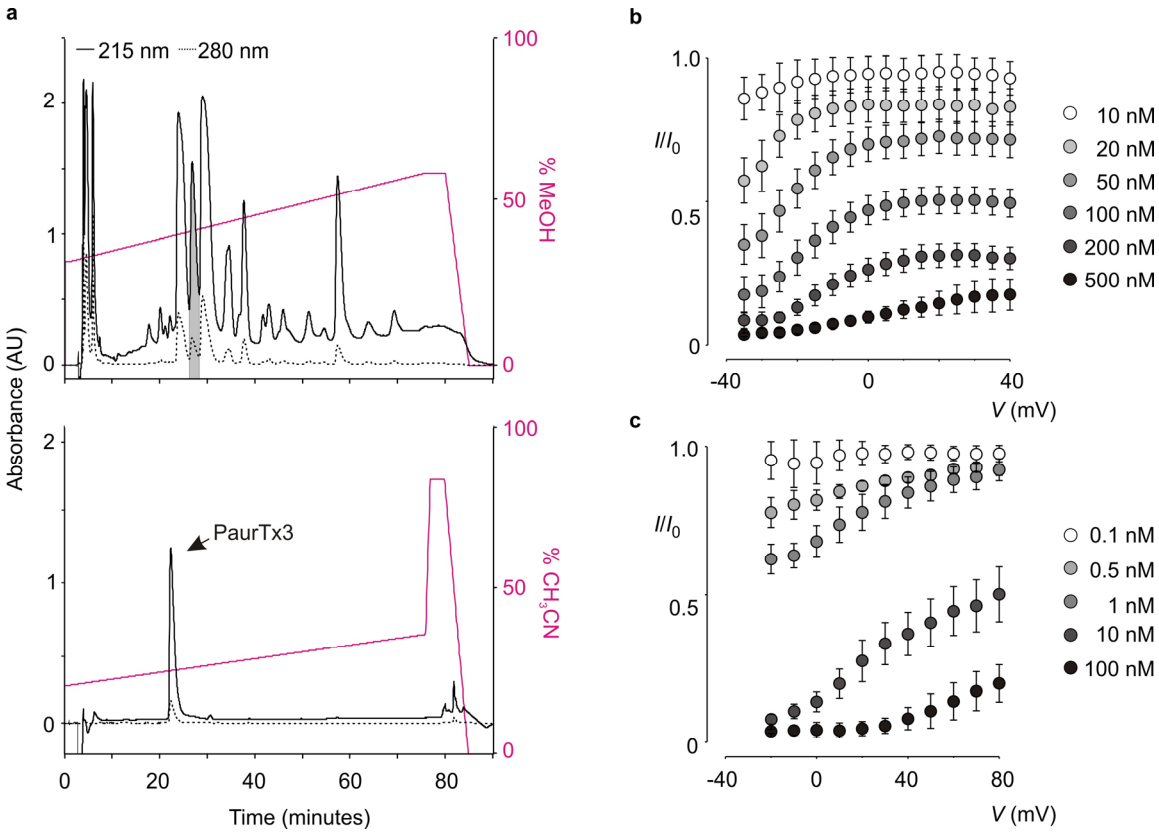

Supplementary Figure 5: Purification of PaurTx3 and measurement of apparent affinity for rNav1.2a and the domain II paddle chimaera. a, PaurTx3 purification from *Phrixotrichus auratus* venom (Spider pharm) in two steps: 1) buffer H_2O/CF_3COOH (0.1%) with a 35% to 60% methanol (MeOH) gradient; 2) buffer H_2O/CF_3COOH (0.1%) with a 20% to 30% acetonitrile (CH_3CN) gradient. The shaded peak in the first step was manually collected and further purified in the second step. Gradients are shown in magenta. System/column: Beckman-Coulter Gold System/C_{18} with UV detection at 215nm and 280nm simultaneously. Flow rate was 1 ml/min. **b-c,** Voltage-dependent inhibition of rNav1.2a (b) and the DII chimaera (c) by PaurTx3 over a range of concentrations. I/I_0 is the fraction of uninhibited current elicited by depolarization to the indicated voltage (V). For rNav1.2a peak test currents were measured, while for the DII chimaera tail currents were measured. The values of I/I_0 measured in the plateau phase at negative voltages where toxin-bound channels do not open were taken as the fraction unbound (Fu).